



3 4456 0368233 4

ORNL/TM-12148

oml

**OAK RIDGE  
NATIONAL  
LABORATORY**

**MARTIN MARIETTA**

**Resolution of Dose and Reduction  
Factor Questions in Army Puise  
Radiation Facility Experiments:  
Renormalization of Calculated  
and Measured Data**

R. T. Santoro  
J. D. Drischler  
J. O. Johnson

OAK RIDGE NATIONAL LABORATORY  
CENTRAL RESEARCH LIBRARY  
CIRCULATION SECTION  
4900N ROOM 125  
**LIBRARY LOAN COPY**  
DO NOT TRANSFER TO ANOTHER PERSON  
If you wish someone else to see this  
report, send in name with report and  
the library will arrange a loan.  
POWERED UP/TH

MANAGED BY  
MARTIN MARIETTA ENERGY SYSTEMS, INC.  
FOR THE UNITED STATES  
DEPARTMENT OF ENERGY

This report has been reproduced directly from the best available copy.

Available to DOE and DCE contractors from the Office of Scientific and Technical Information, P.O. Box 62, Oak Ridge, TN 37831; prices available from (615) 576-8401, FTS 626-8401.

Available to the public from the National Technical Information Service, U.S. Department of Commerce, 5285 Port Royal Rd., Springfield, VA 22161

This report was prepared as an account of work sponsored by an agency of the United States Government. Neither the United States Government nor any agency thereof, nor any of their employees, makes any warranty, express or implied, or assumes any legal liability or responsibility for the accuracy, completeness, or usefulness of any information, apparatus, product, or process disclosed, or represents that its use would not infringe privately owned rights. Reference herein to any specific commercial product, process, or service by trade name, trademark, manufacturer, or otherwise, does not necessarily constitute or imply its endorsement, recommendation, or favoring by the United States Government or any agency thereof. The views and opinions of authors expressed herein do not necessarily state or reflect those of the United States Government or any agency thereof.

U.S. 100  
200 100

**RESOLUTION OF DOSE AND REDUCTION FACTOR  
QUESTIONS IN ARMY PULSE RADIATION FACILITY  
EXPERIMENTS: RENORMALIZATION OF CALCULATED  
AND MEASURED DATA**

**R. T. Santoro  
J. D. Drischler  
J. O. Johnson**

**DATE PUBLISHED - November 1992**

**Prepared by the  
Oak Ridge National Laboratory  
Oak Ridge, Tennessee 37831  
managed by  
MARTIN MARIETTA ENERGY SYSTEMS, INC.  
for the  
U.S. DEPARTMENT OF ENERGY  
under contract DE-AC05-84OR21400**





## CONTENTS

LIST OF FIGURES .....	v
LIST OF TABLES .....	vii
ABSTRACT .....	ix
I. INTRODUCTION .....	1
II. DETAILS OF THE EXPERIMENTS AND ANALYSES .....	2
III. RENORMALIZATION AND COMPARISONS OF MEASURED AND CALCULATED DATA .....	5
IV. CONCLUSIONS AND RECOMMENDATIONS .....	17
REFERENCES .....	18



## LIST OF FIGURES

<u>Figure</u>		<u>Page</u>
1.	Pulse Height versus Pulse Shape for an NE-213 Detector Operating with a Cross-Over Pickoff Pulse Shape Discriminator .....	8
2.	Relative Importance of the FF Gamma-Ray Contributions to the Spectra in the M1A1 and BMP Measurements and in the MASH Calculations .....	12



## LIST OF TABLES

	<u>Table</u>	<u>Page</u>
1.	Detectors Used in the APRF Measurements: Operating Parameters . . . . .	2
2.	Calculated and Measured Fast Neutron and Gamma-Ray Free-Field Doses. Distance from Reactor-to-Detector = 400m . . . . .	5
3.	Free-Field Fast Neutron Normalization Factors, $N_i^{FF}$ for $E_L = 820$ keV . . . . .	7
4.	Fast Neutron Dose and Reduction Factors versus Energy Threshold. Comparison of MASH Results with APRF NE-213 Measurements. Distance from Reactor-to-Detector = 400m . . . . .	10
5.	Gamma-Ray Dose and Reduction Factors versus Energy Threshold. Comparison of MASH Results with APRF NE-213 Measurements. Distance from Reactor- to-Detector = 400m . . . . .	11
6.	"Adjusted" Gamma-Ray Dose and Reduction Factors versus Energy Threshold. Comparison of MASH Results with APRF NE-213 Measurements. Distance from Reactor-to-Detector = 400m . . . . .	14
7.	Free-Field Total Neutron Normalization Factors, $N_i^{FF}$ for $E_L =$ Thermal . . . . .	15
8.	Total Neutron Dose and Reduction Factors. Comparison of MASH Results with APRF NE-213/BF <sub>3</sub> Measurement. Distance from Reactor- to-Detector = 400m . . . . .	16
9.	Total Gamma-Ray Dose and Reduction Factors. Comparison of MASH Results with APRF NE-213 Measurement. Distance from Reactor-to-Detector = 400M	16
10.	"Adjusted" Total Gamma-Ray Dose and Reduction Factors. Comparison of MASH Results with APRF NE-213. Measurement Distance from Reactor-to-Detector = 400m . . . . .	16



## ABSTRACT

A procedure is introduced to normalize calculated and measured dose and reduction factors for a series of experiments performed at the Army Pulse Radiation Facility. In an attempt to isolate causes of the differences among these data, the data are reevaluated on the basis that the free-field neutron and gamma-ray fluence at 400 m from the reactor should be constant within air and ground moisture conditions. When the dose data are compared relative to the number of free-field neutrons, significant improvements are realized in the calculated-to-measured data ratios. Discrepancies in previously reported results appear to be traceable to differences in the number of free-field neutrons and the  $\gamma/n$  ratio at the measurement location.



## I. INTRODUCTION

A series of experiments have been carried out at the Army Pulse Radiation Facility (APRF) to obtain measured data for benchmarking the Adjoint Monte Carlo Shielding Code System, MASH.<sup>(1)</sup> This code system was developed as the principal analytic tool for the U.S. Army for estimating the effects of nuclear weapon radiation on personnel and equipment in armored vehicles and other shielded assemblies. In the experiments, free-field (FF) and in-assembly neutron and gamma-ray spectra and doses were measured at the NATO Standard Reference Distance at 400 m from the reactor. In the analyses, these data are calculated using MASH with the radiation source, terrain features, air and soil moisture content, and the test assembly accurately modeled.

In this paper, the results of an investigation to identify sources of differences among the measured and calculated spectra and doses for four different experiments are presented and discussed. The motivation for this work is based on the premise that since the experiments were carried out under very nearly the same conditions, the measured and calculated FF neutron doses should be very consistent among the experiments and essentially independent of when the experiments were performed. This study focuses on measured data acquired by experimentalists at the APRF and calculated data obtained by analysts from the Oak Ridge National Laboratory (ORNL).

Details of the experiments, procedures used to measure neutron and gamma-ray spectra and dose, and the particulars of the calculations using the MASH code system are given in Section II. The methods used to reassess the measured and calculated data and compare the results on a consistent basis are discussed in Section III. Conclusions and recommendations are presented in Section IV.

## II. DETAILS OF THE EXPERIMENTS AND ANALYSES

The purpose of the experiments conducted at APRF was to obtain differential and integral data for benchmarking and validating the MASH code system over the range of neutrons and gamma-ray energies from thermal to 20 MeV in both the free-field and inside shielded assemblies. To accomplish this, four different assemblies were studied: the Soviet Armored Fighting Vehicle (BMP),<sup>(2,3)</sup> the U.S. Army Abrams Tank (M1A1),<sup>(4,5)</sup> and two steel-walled assemblies, the Radiological Test Configuration (RTK)<sup>(6)</sup> and the Two-Meter Box Test-Bed Assembly (BOX).<sup>(7)</sup> In the BMP and M1A1 experiments, the goal was to measure neutron and gamma-ray doses to determine the reduction and protection factors afforded by the vehicle armor. In the experiments using the two steel-shielded assemblies, the objective was to collect a more extensive neutron and gamma-ray spectra and dose data base for evaluating the broader range of capabilities of the MASH code system in replicating the measurements. Complete details of these experiments including descriptions of the armored vehicles and the steel assemblies may be found in the references. Only those aspects of the measurements and calculations necessary for illuminating the results presented here are included.

Free-field and in-assembly neutron and gamma-ray spectra and doses were acquired using several detectors to cover the range of neutron and gamma-ray energies between thermal and 20 MeV. The detectors and the ranges over which they were operated are given in Table 1. The NE-213 liquid scintillator detector, used primarily to measure fast neutrons ( $E_n > 600$  keV) and secondary gamma-rays ( $E_\gamma > 300$  keV), was operated using pulse-shape discrimination methods to separate neutron and gamma-ray signals in the detector. The NE-213 detector was also used in combination with a  $\text{BF}_3$  detector to measure neutrons over the energy range from thermal to 10 MeV. The  $\text{BF}_3$  detector accounted for the thermal neutron flux while the NE-213 measured the fast neutron flux.

Table 1.  
Detectors Used in the APRF Measurements: Operating Parameters

Detector	Neutron Energy Range	Gamma-Ray Energy Range
NE-213 Liquid Scintillator	$600 \text{ keV} < E_n < 10 \text{ MeV}$	$300 \text{ keV} < E_\gamma < 9 \text{ MeV}$
Tissue Equivalent Ionization Chamber + Geiger-Mueller Counter	$1 \text{ keV} < E_n < 20 \text{ MeV}$	$10 \text{ keV} < E_\gamma < 20 \text{ MeV}$ .
$\text{BF}_3/\text{NE-213}$ Detector Combination	Thermal $< E_n < 10 \text{ MeV}$	

The neutron flux between these energy bounds was inferred using a power function to connect the thermal flux with the low energy cutoff of the NE-213 spectrum. The fit was obtained using

$$f(E) = AE^{-b} . \quad (1)$$

The best correspondence between the two energy bounds was achieved using a value of  $b \approx 0.95$ .

The tissue equivalent ionization chamber and Geiger-Mueller counter combination was used to measure the neutron and gamma-ray dose over the total energy range from 1 keV to 20 MeV.

In each experiment, the measurements were performed in two phases: free-field (FF) and in-assembly. In the FF experiments, the detectors were positioned 400 m from the reactor at a height of 1-m and at a distance of approximately 10 m from the test assembly. In all of the experiments, the test assembly was present during the FF measurements. In the FF, the neutrons emitted directly from the reactor along with secondary gamma-rays from neutron reactions in the intervening air and soil were measured. In the in-assembly investigations, these same radiation modes were measured but with the attenuation of the vehicle or assembly structure (armor) taken into account. Also measured were the gamma-rays produced from incident neutron reactions in the assembly structure. The dose results obtained from the combined measurements are used to determine the radiation reduction and protection factors afforded by the armor. In both phases of the experiments, energy dependent fluence distributions were also acquired.

The calculations using the MASH code system were performed using detailed representation of the APRF leakage spectrum, air and soil moisture conditions, and the vehicles and assemblies. The FF environment was calculated using two-dimensional, discrete ordinates methods in an r-z geometry. The air-over-ground model employed a 240 direction angular quadrature, a  $P_5$  Legendre expansion of the scattering cross-sections, and the DABL69<sup>(8)</sup> (46n,23γ) radiation transport cross-section library. The free-field calculations were carried out using the same air and soil moisture that were present at the time of the measurements.

The adjoint Monte Carlo transport calculations were performed using detailed combinatorial geometry representations of the vehicles or steel assemblies. The calculations generated and tracked a sufficient particle population to assure acceptable statistical uncertainty ( $\pm 1-5\%$ ) in the estimated integral neutron fluence at the detector location. The statistical fluctuations in the fluence per unit energy (spectral data) varied with energy group but were generally within acceptable limits ( $\pm 10\%$ ). An energy dependent importance factor was used to increase the frequency of sampled adjoint source particles from the energy groups having the most effect on the dose response function. Region dependent and energy independent splitting and Russian Roulette techniques were employed to improve the

efficiency of the Monte Carlo calculation and to reduce the statistical fluctuations in the results. The doses were computed by folding the FF and in-assembly fluences with the free-in-air flux-to-dose response functions from DABL69.

### III. RENORMALIZATION AND COMPARISONS OF MEASURED AND CALCULATED DATA

A concern that arises when the measured and calculated FF neutron doses are examined for the four experiments is the discrepancy among and between the results. Table 2 summarizes the fast neutron ( $E_n > 600$  keV) and secondary gamma-ray doses reported by investigators from APRF and ORNL. The M1A1 fast neutron spectra are for energies  $E_n > 800$  keV. The columns labeled C summarize the calculated doses for the air-soil conditions, detector type, and detector operating range used to determine the measured results, M.

Although the experiments were performed at different times, the conditions at the APRF were very nearly the same. The differences among the data cannot, for example, be accounted for on the basis of atmospheric or soil moisture conditions. Johnson, et. al.<sup>(9)</sup> and Kaul and Egbert<sup>(10)</sup> have shown that the variations in the calculated FF doses at the 400 m location vary by less than 5% over the range of air and soil moisture conditions normally encountered at the APRF site. Even for extreme moisture conditions, the calculated doses vary by only 13%. The differences in the calculated data in Table 2, however, are as much as 33% while the measured data fluctuate by as much as 44%. The differences in the secondary gamma-ray doses are 22% between the calculated data and 24% between the measured data.

Table 2  
Calculated and Measured Fast Neutron and Gamma-Ray Free-Field Doses.  
Distance from Reactor-to-Detector = 400m

Experiment	C	M	CM
<u>Fast Neutron Dose-FF</u> (mrad/kWh)			
BMP	3.93	2.98	1.32
M1A1	2.94	2.16	1.36
RTK	3.78	2.07	1.83
BOX	3.72	2.28	1.63
<u>Gamma-Ray Dose-FF</u> (mrad/kWh)			
BMP	1.34	1.24	1.08
M1A1	1.30	1.49	0.87
RTK	1.17	1.31	0.89
BOX	1.10	1.54	0.71

When the neutron doses are compared in terms of the calculated-to-measured (C/M) ratio, the differences between the measured and calculated data are as large as 83%. The C/M ratios indicate differences between the calculated and measured gamma-ray doses as large as 29%. For these studies, the Defense Nuclear Agency has defined the criterion for acceptability of MASH in reproducing the experiment as  $\pm 20\%$ . The data results summarized in Table 2 suggest that there may be difficulties in the measurements, calculations, or both. Other sources of the differences may be due to the interpretation of detector threshold or the normalization of the data with respect to reactor power, operating times, etc.

In an attempt to account for the differences in the data, the following assumptions have been adopted in reassessing the measured and calculated results. The main assumption is that the neutron yield per unit of reactor power is constant in all of the experiments. Consequently, if an ideal neutron detector is placed at a distance of 400 m from the reactor and sufficiently far from the armored vehicle or test assembly so that the spectrum is not perturbed by the structure, then the spectrum measured at this location should be constant within the differences introduced by fluctuations in atmospheric and soil moisture content. To normalize the data on a consistent basis, the following procedure was adopted.

For each experiment, the measured and calculated fast and total neutron free-field energy dependent fluence (spectra),  $\phi_i^{FF}(E)$  were each normalized to the total number of neutrons that contributed to the free-field fluence. The number of free-field neutrons,  $N_i^{FF}(E \geq E_L)$ , was calculated using

$$N_i^{FF}(E \geq E_L) = \int_{E_L}^{E_U} \phi_i^{FF}(E) dE, \quad i = m, c. \quad (2)$$

where the subscript i indicates measured (m) or calculated (c) data. The limits of integration signify the energy range over which the number of fast free-field neutrons are determined. The basis for setting the limits in the normalization is discussed below. The differential neutron and gamma-ray fluences were then renormalized using

$$\Phi_{i,j}^k(E) = \phi_{i,j}^k(E) / N_i^{FF}(E \geq E_L) \quad (3)$$

where the superscript k denotes the free-field or in-assembly fluence and the subscript j indicates neutrons or gamma-rays. Finally, the measured and calculated dose were recomputed by folding the normalized fluence  $\Phi_{i,j}^k(E)$  with the appropriate flux-to-dose conversion factor  $R_j(E)$  using

$$D_{i,j}^k(E \geq E_L) = \int_{E_L}^{E_U} \Phi_{i,j}^k(E) R_j(E) dE. \quad (4)$$

The FF and in-assembly doses obtained using Equation 4, are normalized to the number of free-field neutrons with energies  $\geq E_L$  calculated using Equation 2. The fast neutron and gamma-ray doses obtained with Equation 4 were calculated for different energy threshold values,  $E_L$ . The total dose data were computed for  $E_L = \text{thermal}$ .

It appears likely the measured neutron and gamma-ray spectra were obtained over energy limits (See Table 1) that are beyond the capability of an NE-213 detector system. Figure 1 plots the pulse height (energy) versus pulse-shape (channel number) dependence of neutrons and gamma-rays separated using a cross-over pickoff pulse-shape discriminator (PSD). These data were obtained at ORNL using a 5-cm diameter by 5-cm-high NE-213 detector and a  $^{252}\text{Cf}$  neutron source. The point to note from these data is the shift in the neutron distributions with increasing energy. At energies above 800 keV, the neutron distributions shift toward higher channel number while the gamma-ray distributions remains relatively constant with channel number. At energies below 800 keV, the gamma-ray distributions shift towards lower channel number. Because of this behavior, considerable care must be taken in setting both the lower energy neutron and PSD bias levels to assure optimum n- $\gamma$  separation over the operating range of the detector and to assure that the neutron spectra are not contaminated by gamma-ray pulses, and vice versa. Setting the energy bias too low will result in loss of information, as well as misinformation, in the neutron and gamma-ray pulse height spectra. In this analysis, the assumption was made that the PSD system used with the APRF NE-213 detector exhibits the same behavior as shown in Figure 1.

In renormalizing the measured and calculated data, the low energy cutoff for the fast neutrons was taken to be 820-keV. At this bias and further assuming that the PSD is set similar to that indicated in Figure 1, the neutron or gamma-ray spectra should be adequately resolved. The normalization factors for the measured and calculated fast neutron fluence determined using Equation 2 with  $E_L = 820 \text{ keV}$  and  $E_U = 10 \text{ MeV}$  are summarized in Table 3. A value of  $1.29 \times 10^{17}$  neutrons per kWh was used in Equation 2 to compute the normalization factors for the calculated data.

Table 3  
Free-Field Fast Neutron Normalization Factors,  $N_i^{FF}$  for  $E_L = 820 \text{ keV}$

Experiment	Calculated Data	Measured Data
BMP	$9.71 \times 10^5$	$6.27 \times 10^5$
M1A1	$9.52 \times 10^5$	$3.21 \times 10^6$
RTK	$1.13 \times 10^6$	$6.20 \times 10^5$
BOX	$9.92 \times 10^5$	$6.65 \times 10^5$

The renormalized FF and in-assembly fast neutron and secondary gamma-ray doses and reduction factors for the four experiments are presented in Tables 4 and 5, respectively. The data are presented as a function of detector threshold energy.

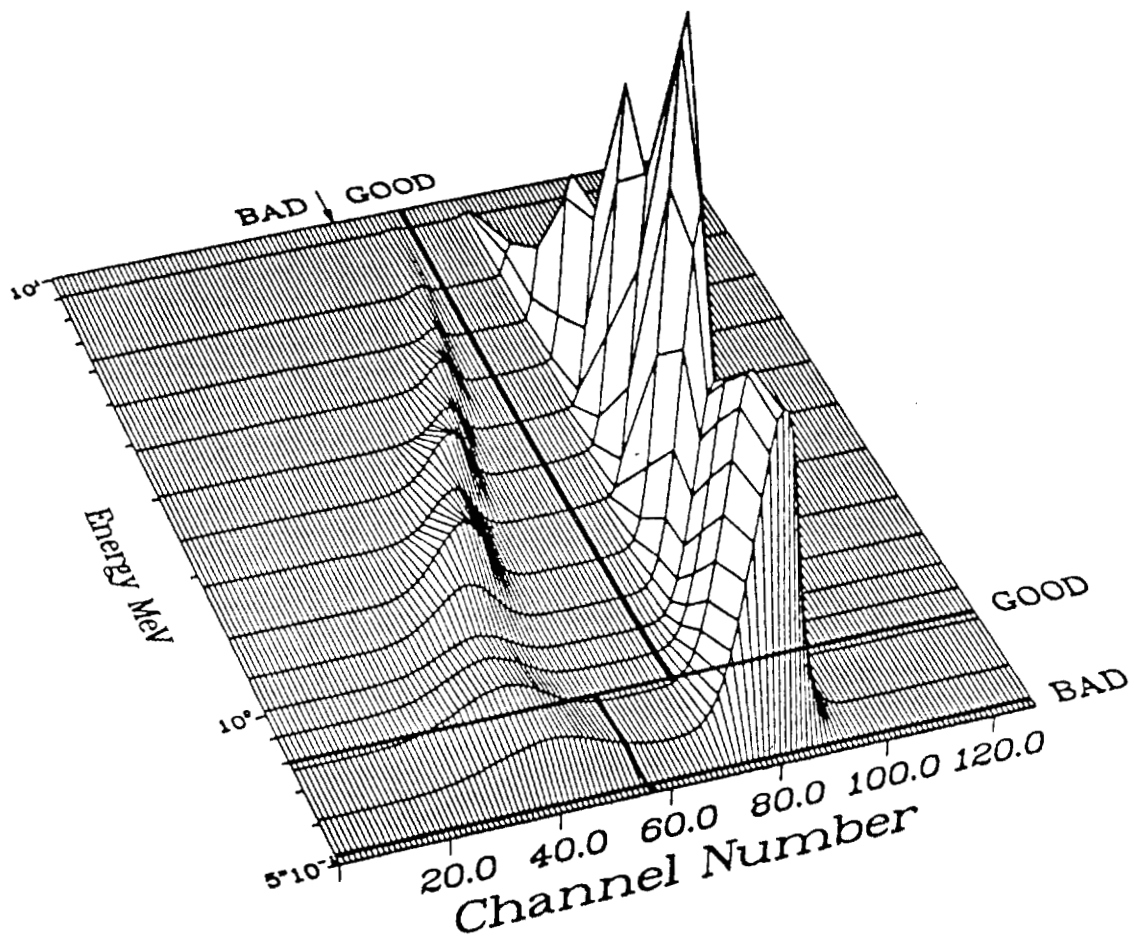


Figure 1. Pulse Height versus Pulse Shape for an NE-213 Detector Operating with a Cross-Over Pickoff Pulse Shape Discriminator

The fast neutron data summarized in Table 4 were calculated using Equation 4 as a function of threshold energies,  $E_T$ , of 0.820, 0.961, 1.10, and 1.82 MeV.\* These energy values correspond to the neutron energy group boundaries in the DABL69 cross-section library. To assure that the measured and calculated data were compared on the same basis, the measured data were rebinned into the DABL69 energy group structure prior to renormalization. The FF doses, in units of Gray per  $N_i^{FF}$  neutrons are now in good agreement among and between the calculations and measurements for the four experiments. The agreement between the calculated FF data is of the order of 2% at all threshold energies. The agreement between the measured data is within 7% for threshold energies of 820 and 961 keV and 14%, or less, at the higher threshold energies. The C/M ratios of the FF dose indicate good agreement (10%) between calculated and measured doses except for the M1A1 and BOX doses above a threshold of 1.82 MeV, where the agreement increases to about 15%. The C/M ratios for the in-assembly doses show marked improvement over the results reported in the references and, with the exception of the BMP experiment, are within 10-20%. For the BMP, the calculation consistently underestimates the measurement by 50%, or more. The calculation reproduces the neutron reduction factor (NRF) to better than  $\pm 20\%$  for all of the assemblies, except the BMP where the NRF is consistently underestimated by about 30% which is expected because of the disparity in the calculated and measured in-vehicle doses.

The renormalized gamma-ray data summarized in Table 5 reveal some very interesting behavior. The data were calculated for detector threshold energies of 0.70, 1.00, 1.50, and 2.00 MeV which correspond to the gamma-ray energy boundaries in DABL69. The agreement between calculated FF gamma-ray doses is within 6% among the experiments at all threshold energies. The measured FF doses, on the other hand, exhibit a large spread among the data for the four experiments. The differences between the BMP, RTK, and BOX free-field doses are as large as 30% while the FF gamma-ray dose in the M1A1 experiment is consistently greater than all other data by a factor of approximately two.

The difference between calculated and measured FF gamma-ray doses can be attributed to two causes. In the experiments, the FF dose is measured with the detectors located at 400-m from the reactor at a distance of approximately ten meters from the test assembly. As a result, the measured FF photon dose is due both to gamma-rays produced in neutron reactions in the air and ground, as discussed above, and a gamma-ray contribution from 7.2 MeV gamma-rays from thermal neutron capture in iron in the experimental assemblies. The fraction of the capture gamma-ray contribution to the dose is roughly proportional to the mass of iron in the assembly which is in the proportion BMP:RTK:BOX:M1A1. The M1A1, however, is extremely heavy compared to the other assemblies and is constructed almost entirely of iron and considerably perturbs the FF gamma-ray measurements. Figure 2 compares the relative contribution of photons with energy  $E_\gamma$  to the FF gamma-ray fluence measured in the M1A1 and BMP experiments with calculated results obtained with MASH. At energies below 7 MeV, all of the spectra are similar in shape and magnitude and the differences among the data have a small impact on the integral spectra and dose. At energies above 7 MeV, the M1A1 data show a large contribution to the spectrum compared to the BMP and MASH cases. In this energy region, the flux-to-dose response is large so the dose is dominated by the large fraction of capture gamma radiation due to the presence of the tank.

---

\*Some columns in this and other tables have been left blank because the data are classified.

Table 4  
Fast Neutron Dose and Reduction Factors versus Energy Threshold  
Comparison of MASH Results with APRF NE-213 Measurements  
Distance from Reactor-to-Detector = 400m.

SYSTEM	CALCULATED			MEASURED			(C/M) <sub>FF</sub>	(C/M) <sub>IN</sub>	(C/M) <sub>RF</sub>
	Dose-FF	Dose-IN	NRF	Dose-FF	Dose-IN	NRF			
	Gy/N <sub>c</sub> <sup>FF</sup>	Gy/N <sub>c</sub> <sup>FF</sup>		Gy/N <sub>m</sub> <sup>FF</sup>	Gy/N <sub>m</sub> <sup>FF</sup>				
E <sub>n</sub> > 820 keV									
BMP	3.11-11			3.11-11			1.00	1.49	0.68
M1A1	3.10-11			3.26-11			0.95	1.19	0.80
RTK	3.11-11	1.44-12	21.6	3.10-11	1.30-12	23.9	1.00	1.11	0.91
BOX	3.09-11	9.22-12	3.35	3.23-11	8.96-12	3.60	0.96	1.03	0.93
E <sub>n</sub> > 961 keV									
BMP	2.78-11			2.88-11			0.97	1.44	0.67
M1A1	2.77-11			3.06-11			0.91	1.09	0.83
RTK	2.75-11	1.19-12	23.1	2.85-11	1.13-12	25.22	0.96	1.05	0.92
BOX	2.76-11	7.58-12	3.64	2.99-11	7.83-12	3.82	0.92	0.97	0.95
E <sub>n</sub> > 1.10 MeV									
BMP	2.59-11			2.61-11			0.99	1.51	0.66
M1A1	2.58-11			2.87-11			0.90	0.99	0.91
RTK	2.56-11	1.04-12	24.6	2.55-11	9.44-13	2.70	1.00	1.10	0.91
BOX	2.56-11	6.58-12	3.89	2.77-11	6.82-12	4.06	0.92	0.96	0.96
E <sub>n</sub> > 1.82 MeV									
BMP	1.70-11			1.62-11			1.05	1.65	0.64
M1A1	1.68-11			2.06-11			0.82	0.83	0.98
RTK	1.65-11	5.14-13	32.1	1.53-11	4.86-13	31.5	1.08	1.06	1.02
BOX	1.66-11	3.24-12	5.12	1.95-11	3.83-12	5.09	0.85	0.85	1.01

Table 5

Gamma-Ray Dose and Reduction Factors versus Energy Threshold  
 Comparison of MASH Results with APRF NE-213 Measurements  
 Distance from Reactor-to-Detector = 400m.

SYSTEM	CALCULATED			MEASURED			(C/M) <sub>FF</sub>	(C/M) <sub>IN</sub>	(C/M) <sub>RF</sub>
	Dose-FF	Dose-IN	GRF	Dose-FF	Dose-IN	GRF			
	Gy/N <sub>c</sub> <sup>FF</sup>	Gy/N <sub>c</sub> <sup>FF</sup>		Gy/N <sub>m</sub> <sup>FF</sup>	Gy/N <sub>m</sub> <sup>FF</sup>				
$E_\gamma > 700 \text{ keV}$									
BMP	1.07-11			1.60-11			0.67	0.58	1.15
M1A1	1.07-11			3.69-11			0.29	0.23	1.24
RTK	1.05-11	2.20-12	4.77	1.79-11	3.16-12	5.66	0.56	0.70	0.84
BOX	1.01-11	3.07-12	3.29	1.88-11	4.64-12	4.05	0.54	0.66	0.81
$E_\gamma > 1.00 \text{ MeV}$									
BMP	9.96-12			1.48-11			0.67	0.58	1.15
M1A1	9.94-12			3.48-11			0.29	0.23	1.22
RTK	9.78-12	2.18-12	4.49	1.67-11	3.02-12	5.53	0.59	0.72	0.84
BOX	9.44-12	2.84-12	3.32	1.77-11	4.36-12	4.06	0.53	0.65	0.82
$E_\gamma > 1.50 \text{ MeV}$									
BMP	8.83-12			1.28-11			0.69	0.58	1.18
M1A1	8.81-12			3.13-11			0.28	0.24	1.19
RTK	8.64-12	1.96-12	4.41	1.47-11	2.84-12	5.18	0.59	0.69	0.85
BOX	8.40-12	2.63-12	3.19	1.59-11	4.06-12	3.92	0.53	0.65	0.81
$E_\gamma > 2.00 \text{ MeV}$									
BMP	7.73-12			1.00-11			0.77	0.60	1.29
M1A1	7.69-12			2.72-11			0.28	0.24	1.19
RTK	7.48-12	1.81-12	4.13	1.21-11	2.65-12	4.57	0.62	0.68	0.90
BOX	7.38-12	2.41-12	3.06	1.42-11	3.75-12	3.79	0.52	0.64	0.81

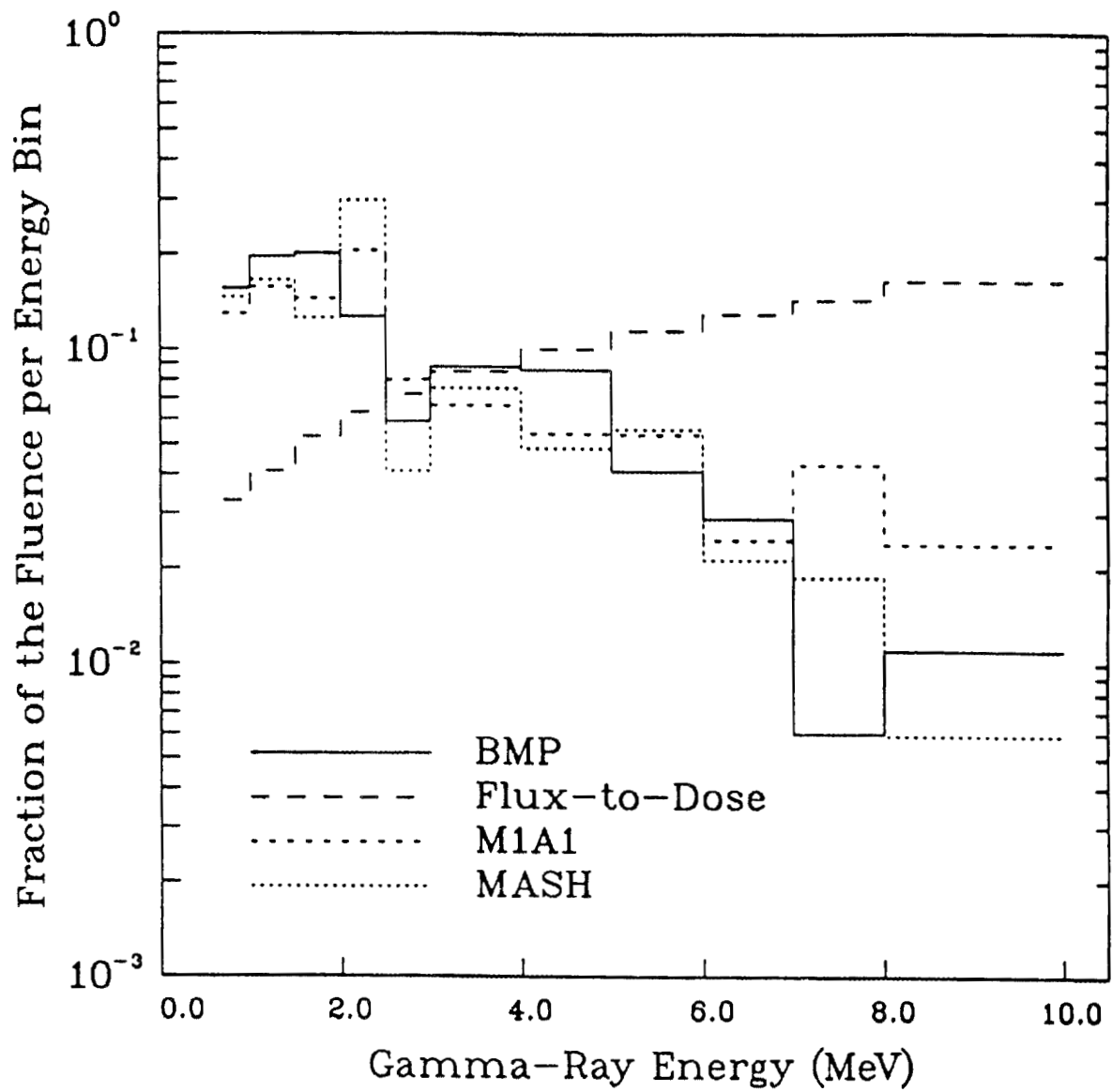


Figure 2. Relative Importance of the FF Gamma-Ray Contributions to the Spectra in the M1A1 and BMP Measurements and in the MASH Calculations

Further examination of the calculated and measured FF gamma-ray doses reveals another interesting trend. The FF dose C/M ratios show that the calculation consistently underestimates the measurement (ignoring the M1A1 case) by nominally 35-45%. Taking the ratio of the FF gamma-ray to FF neutron dose of both the calculated and measured data (which corresponds approximately to the number of photons per neutron) reveals that the calculations yield a  $\gamma/n$  ratio of  $\sim 0.34$  while the measurements show the ratio to be  $\sim 0.56$ , or a difference of about 65%.

Kaul and Egbert<sup>(11)</sup> performed extensive calculations to estimate the  $\gamma/n$  for the APRF reactor and determined this value to be 0.39 which is the value used in the MASH calculations. There appears, however, to be an additional gamma radiation source in the measured results that are not being appropriately accounted for in the MASH analysis. There has been considerable speculation among the analysts and experimentalists that the trees in the vicinity of the 400 m site or an oil-filled transformer housed in a building adjacent to the reactor building and ostensibly in the path of the source neutrons migrating from the reactor to the 400-m test site may produce this "extra" component of gamma radiation. If the photons emanate from the trees, then the measured gamma-ray spectra should contain a substantial fraction of 2.2 MeV photons from neutron reactions in the hydrogen contained in the trees. The fraction of the measured FF gamma-ray dose above 700 keV from 2.2-MeV photons is 15% in the BMP, RTK, and BOX measurements. While this is not an insignificant contribution, the trees do not appear to be the primary source of the inconsistency between the measured and calculated FF gamma-ray doses. A more likely cause is the several tons of oil in the tank. Neutron reactions in the hydrogen and carbon in the oil will produce large quantities of 2.2 and 4.3 MeV gamma-rays not to mention photons produced in the tank and the surrounding building. These gamma-rays will change the  $\gamma/n$  ratio in the free-field from that predicted in Reference 11.

Assuming that the gamma-ray fluence is higher than previously predicted, then the calculated free-field gamma doses can be scaled by the ratio  $(\gamma/n)_M/(\gamma/n)_C = 1.65$ . Correspondingly, because the BMP, RTK, and BOX are relatively thin assemblies, the scaling may also be applied to the in-system doses. The "adjusted" calculated data for these assemblies are compared with the measured data in Table 6. The agreement between the calculated and measured doses are considerably improved. Scaling the calculated data in this manner is speculative and is intended principally to illustrate the effects of the differences in the  $\gamma/n$  ratio. A problem does, however, exist in the magnitude of the gamma-ray component that is used in the calculations and appears to be due to the omission in the calculations of the oil-filled tank and structure and, to a lesser extent, the trees.

No attempt was made to adjust the M1A1 dose data. The mass of the tank is so great that the gamma-ray environment in the free-field at detector locations in the vicinity of the tank are dramatically perturbed. The calculation should be repeated with the tank included or the experiment rerun with the tank absent to obtain a more consistent comparison of the results.

The same approach used to study the fast neutron and gamma-ray data was also employed to analyze differences between the calculated and measured total neutron and gamma-ray doses. Measured total dose data, obtained using the NE-213/BF<sub>3</sub> detector combination, were available only for the BMP and RTK experiments. The differential spectra

Table 6

"Adjusted" Gamma-Ray Dose and Reduction Factors versus Energy Threshold  
 Comparison of MASH Results with APRF NE-213 Measurements  
 Distance from Reactor-to-Detector = 400m.

SYSTEM	CALCULATED			MEASURED			(C/M) <sub>FF</sub>	(C/M) <sub>IN</sub>	(C/M) <sub>RF</sub>
	Dose-FF	Dose-IN	GRF	Dose-FF	Dose-IN	GRF			
	Gy/n	Gy/n		Gy/n	Gy/n				
$E_{\gamma} > 700 \text{ keV}$									
BMP	1.77-11			1.60-11			1.11	0.96	1.16
RTK	1.73-11	3.63-12	4.77	1.79-11	3.16-12	5.66	0.97	1.15	0.84
BOX	1.67-11	5.07-12	3.29	1.88-11	4.64-12	4.05	0.89	1.09	0.81
$E_{\gamma} > 1.00 \text{ MeV}$									
BMP	1.62-11			1.48-11			1.09	0.96	1.14
RTK	1.61-11	3.60-12	4.47	1.67-11	3.02-12	5.53	0.96	1.19	0.81
BOX	1.56-11	4.69-12	3.32	1.77-11	4.36-12	4.06	0.88	1.08	0.82
$E_{\gamma} > 1.50 \text{ MeV}$									
BMP	1.46-12			1.28-11			1.14	0.96	1.18
RTK	1.43-12	3.23-12	4.41	1.47-11	2.84-12	5.18	0.97	1.14	0.85
BOX	1.39-12	4.34-12	3.19	1.59-11	4.06-12	3.92	0.87	1.09	0.81
$E_{\gamma} > 2.00 \text{ MeV}$									
BMP	1.28-12			1.00-11			1.28	0.98	1.31
RTK	1.23-12	2.99-12	4.13	1.21-11	2.65-12	4.57	1.02	1.13	0.91
BOX	1.22-12	3.98-12	3.06	1.42-11	3.75-12	3.79	0.86	1.06	0.86

were normalized using Equation 2 to the total number of neutrons above thermal energy. The normalization factors are listed in Table 7. The recomputed total neutron dose and reduction factor data are given in Table 8. The FF doses for the BMP are in excellent agreement while the corresponding data for the RTK are marginal. The agreement between the calculated and measured in-assembly doses are poor but improved over the values reported in References 2 and 6. No improvement is realized in the neutron reduction factor for the BMP study where the C/M ratio has been consistently poor.

Table 7  
Free-Field Total Neutron Normalization Factors,  $N_i^{FF}$  for  $E_L = \text{Thermal}$

Experiment	Calculated Data	Measured Data
BMP	$7.39 \times 10^6$	$4.57 \times 10^6$
RTK	$9.68 \times 10^6$	$6.14 \times 10^6$

Comparing the ratio of the number of total neutrons to the number of fast neutrons from Tables 3 and 6, respectively, the BMP data yield values of 7.6 for both the calculated and measured data while the RTK ratios are 8.6 and 9.9 for the calculated and measured normalization factors, respectively. This raises a concern as to why the total free-field neutron populations are different in the two studies. One explanation may be the manner in which the thermal and fast portions of the measured data are "connected" using the fitting function given by Equation 2. No attempt was made here to determine the validity of the measured spectra in the transition region between the thermal fluence measured using the  $\text{BF}_3$  detector and the lower energy cutoff off the NE-213 spectrum.

The calculated and measured total gamma-ray doses and reduction factors ( $E_\gamma \geq 300$  keV) are compared in Table 9. As in the case of the FF gamma-ray doses, the C/M ratios for both the FF and in-system comparisons are poor (>20%). The calculated and measured reduction factors are in marginal agreement. In the case of the total doses, the  $\gamma/n$  ratio for the calculated data is 0.22 compared to 0.35 for the measured data. The ratio  $[(\gamma/n)_M/(\gamma/n)_C]$  is 1.61; the same as for the fast data. Adopting the same logic as above, the calculated data in Table 9 have been multiplied by this value to yield the "adjusted" data presented in Table 10. The calculated and measured FF and in-system doses are now in much better agreement although, as expected, the reduction factors remain in only marginal agreement.

Table 8

Total Neutron Dose and Reduction Factors  
 Comparison of MASH Results with APRF NE-213/BF<sub>3</sub> Measurement  
 Distance from Reactor-to-Detector = 400m.

SYSTEM	CALCULATED			MEASURED			(C/M) <sub>FF</sub>	(C/M) <sub>IN</sub>	(C/M) <sub>RF</sub>
	Dose-FF	Dose-IN	NRF	Dose-FF	Dose-IN	NRF			
	Gy/N <sub>c</sub> <sup>FF</sup>	Gy/N <sub>c</sub> <sup>FF</sup>		Gy/N <sub>m</sub> <sup>FF</sup>	Gy/N <sub>m</sub> <sup>FF</sup>				
BMP	6.88-12			6.77-12			1.01	1.50	0.66
RTK	6.50-12	3.94-13	16.7	5.44-12	2.88-13	18.8	1.19	1.36	0.88

Table 9

Total Gamma-Ray Dose and Reduction Factors  
 Comparison of MASH Results with APRF NE-213 Measurement  
 Distance from Reactor-to-Detector = 400m.  
 (E<sub>γ</sub> ≥ 700 keV)

SYSTEM	CALCULATED			MEASURED			(C/M) <sub>FF</sub>	(C/M) <sub>IN</sub>	(C/M) <sub>RF</sub>
	Dose-FF	Dose-IN	GRF	Dose-FF	Dose-IN	GRF			
	Gy/N <sub>c</sub> <sup>FF</sup>	Gy/N <sub>c</sub> <sup>FF</sup>		Gy/N <sub>m</sub> <sup>FF</sup>	Gy/N <sub>m</sub> <sup>FF</sup>				
BMP	1.57-12			2.59-12			0.69	0.59	1.15
RTK	1.41-12	3.50-13	4.02	2.16-12	4.26-12	5.07	0.73	0.83	0.84

Table 10

"Adjusted" Total Gamma-Ray Dose and Reduction Factors  
 Comparison of MASH Results with APRF NE-213 Measurement  
 Distance from Reactor-to-Detector = 400m.  
 (E<sub>γ</sub> ≥ 700 keV)

SYSTEM	CALCULATED			MEASURED			(C/M) <sub>FF</sub>	(C/M) <sub>IN</sub>	(C/M) <sub>RF</sub>
	Dose-FF	Dose-IN	GRF	Dose-FF	Dose-IN	GRF			
	Gy/N <sub>c</sub> <sup>FF</sup>	Gy/N <sub>c</sub> <sup>FF</sup>		Gy/N <sub>m</sub> <sup>FF</sup>	Gy/N <sub>m</sub> <sup>FF</sup>				
BMP	2.52-12			2.59-12			1.14	0.97	1.15
RTK	2.27-12	5.63-13	4.02	2.16-12	4.26-12	5.07	1.20	1.37	0.84

## IV. CONCLUSIONS AND RECOMMENDATIONS

Normalizing the calculated and measured doses and reduction factors using the procedures described above lead to improved C/M ratios and suggest that many of the discrepancies observed among the data may not be as severe as previously reported. Several problems have been identified, however, that must be resolved before dependable comparisons can be realized and the MASH code system can be fully accredited for assessing the full range of spectral and dose issues in armored vehicles.

In general, MASH reproduces the reduction factors to C/M values of  $\pm 20\%$  which are within the limit mandated by the Defense Nuclear Agency as the performance criterion for the code. Doses, on the other hand, are less consistently replicated and, in some cases, the differences are large and the results are unacceptable.

The procedure used here to renormalize the measured and calculated data has revealed a number of issues that should be resolved. A major concern is the difference in the number of free-field neutrons per kWh at 400 m obtained by the experimentalists and analysts. The calculated and measured values in Tables 3 and 7 differ by 60% and 26%, respectively. A consistent value for the fluence as a function of reactor power needs to be defined for normalization of both the calculations and the experiments. Also, to obtain correct comparisons between the gamma-ray data, more precise resolution of the  $\gamma/n$  ratio must also be established.

Detailed analyses of the impact on the calculated results of the oil-filled tank and trees are necessary. This will be easier to accomplish when three-dimensional discrete ordinates procedures are incorporated in the MASH code system to determine the air-over-ground environment and the flux on the coupling surface around the test assembly. Also, the free-field measurements and the calculations must be performed for the same experimental conditions, i.e., with the test assembly present or absent at the 400 m location.

## REFERENCES

1. J. O. Johnson, "A User's Manual for MASH 1.0 - A Monte Carlo Adjoint Shielding Code System", Oak Ridge National Laboratory, ORNL/TM-11778 (March 1992).
2. J. O. Johnson, Oak Ridge National Laboratory, Private Communication.
3. Craig R. Heimbach, U. S. Army Combat Systems Test Activity, Aberdeen Proving Ground, Maryland, Private Communication.
4. J. O. Johnson, Oak Ridge National Laboratory, Private Communication.
5. Craig R. Heimbach, U. S. Army Combat Systems Test Activity, Aberdeen Proving Ground, Maryland, Private Communication.
6. J. O. Johnson, "Analysis of the Radiological Test Configuration (RTK) Experiments Using the Monte Carlo System, - MASH, ORNL/TM-11410, (March 1990).
7. R. T. Santoro, et.al., "DNA Radiation Environments Program Fall 1989 2-Meter Box Experiments and Analysis", Oak Ridge National Laboratory, (May 1991).
8. D. T. Ingersoll, R. W. Roussin, C. Y. Fu, and J. E. White, "DABL69: A Broad Group Neutron/Photon Cross Section Library for Defense Nuclear Applications", Oak Ridge National Laboratory, ORNL/TM-10568, (June 1989).
9. J. O. Johnson, J. D. Drischler, and J. M. Barnes, "Analysis of the Fall 1989 two-Meter Box Test Bed Experiments Performed at the Army Pulse Radiation Facility (APRF)", Oak Ridge National Laboratory, ORNL/TM-11777 (May 1991).
10. Dean C. Kaul and Stephen D. Egbert, Presentation at the 1989 Radiation Environments Program Review, Defense Nuclear Agency, Alexandria, VA.
11. Dean C. Kaul and Stephen D. Egbert, "Radiation Leakage from the Army Pulse Radiation Facility (APRF) Fast Reactor", Science Applications International Corporation, SAIC-89/1423, (May 1989)

INTERNAL DISTRIBUTION

- |                       |   |
|-----------------------|---|
| 1. B. R. Appleton     | 24. R. C. Ward                          |
| 2-6. J. M. Barnes     | 25-26. EPMD Reports Office              |
| 7. T. J. Burns        | 27-28. Laboratory Records<br>Department |
| 8-12. J. D. Drischler | 29. Laboratory Records<br>ORNL-RC       |
| 13. C. M. Haaland     | 30. Document Reference<br>Section       |
| 14. D. T. Ingersoll   | 31. Central Research<br>Library         |
| 15-19. J. O. Johnson  | 32. ORNL Patent Section                 |
| 20. J. V. Pace        |   |
| 21. W. A. Rhoades     |   |
| 22. R. W. Roussin     |   |
| 23. R. T. Santoro     |   |

EXTERNAL DISTRIBUTION

33. Director, Defense Nuclear Agency  
ATTN: RARP (Dr. D. L. Auton)  
6801 Telegraph Road  
Alexandria, VA 22310-3398
34. Dr. Roger W. Brockett  
Wang Professor of Electrical Engineering  
and Computer Science  
Division of Applied Science  
Harvard University  
Cambridge, Massachusetts 02138
35. Electronics Division, NES  
ATTN: Dr. Tom Cousins  
Defence Research Establishment Ottawa  
Ottawa, Ontario, Canada, K1A 0Z4

36. Commander, U.S. Army Nuclear & Chemical Agency  
ATTN: MONA-ZB (Dr. David Bash)  
7500 Backlick Rd., Bldg. 2073  
Springfield, VA 22150-3198
37. Etablissement Technique Central de l' Armement  
ATTN: Dr. Joel Dhermain  
Centre d'Etudes du Boucher  
16 bis Avenue Prieur de la Cote d'or  
94114 Arcueil-Cedex, France
38. Science Applications International Corporation  
ATTN: Dr. Stephen Egbert  
10260 Campus Point Drive  
San Diego, CA 92121
39. Commander, U.S. Army Combat Systems Test Activity  
ATTN: STECS-NE (Mr. John Gerdes)  
Aberdeen Proving Ground, MD 21005-5059
40. Ministry of Defence, Atomic Weapons Establishment  
ATTN: Dr. Kevin G. Harrison  
Building A72, Aldermaston,  
Reading, Berkshire, United Kingdom, RG7 4PR
41. Commander, U.S. Army Combat Systems Test Activity  
ATTN: STECS-NE (Dr. C. Heimbach)  
Aberdeen Proving Ground, MD 21005-5059
42. Director, Bubble Technology Industries, Inc.  
ATTN: Dr. Harry Ing  
Highway 17  
Chalk River, Ontario, Canada, KOJ 1JO
43. Science Applications International Corporation  
ATTN: Mr. Dean C. Kaul  
10260 Campus Point Drive  
San Diego, CA 92121
44. Commander, U.S. Army Combat Systems Test Activity  
ATTN: STECS-NE (Dr. A. Halim Kazi)  
Aberdeen Proving Ground, MD 21005-5059
45. Director, Armed Forces Radiobiology Research Institute  
ATTN: MRAD (CDR Kearsly)  
Bethesda, MD 20814-5145

46. Director, Defense Nuclear Agency  
ATTN: RARP (MAJ Robert Kehlet)  
6801 Telegraph Road  
Alexandria, VA 22310-3398
47. Director, Harry Diamond Laboratory  
ATTN: SLCHD-NW-P (Mr. Klaus Kerris)  
2800 Powder Mill Road  
Adelphi, MD 20783-1197
48. US Army Center for EQ/RSTA  
ATTN: AMSEL-RSK (Dr. Stanley Kronenberg)  
Fort Monmouth, NY 07703
49. Establissement Technique Central de l' Armement  
ATTN: Dr. Jacques Laugier  
Centre d'Etudes du Boucher  
16 bis Avenue Prieur de la Cote d'or  
94114 Arcueil-Cedex, France
50. Dr. James E. Leiss  
Route 2, Box 142C  
Broadway, VA 22815
51. Dr. Neville Moray  
Department of Mechanical and Industrial Engineering  
University of Illinois  
1206 West Green Street  
Urbana, IL 61801
52. Director, Defense Nuclear Agency  
ATTN: RARP (Ms. Joan Ma Pierre)  
6801 Telegraph Road  
Alexandria, VA 22310-3398
53. Naval Surface Warfare Center  
ATTN: CODE R41 (Mr. Gordon Reil)  
New Hampshire Road  
White Oak, MD 20903-5000
54. Commander, U.S. Army Foreign Science & Technology Center  
ATTN: UVA (Dr. Roger Rydin)  
220 7th Street NE  
Charlottesville, VA 22901-5396

55. HEAD, Nuclear Radiation Effects  
ATTN: Dr. Ludwig Schaenzler  
Wehrwissenschaftliche Dienststelle  
Postfach 1320  
3042 Munster  
Federal Republic of Germany
56. Commander, U.S. Army Foreign Science & Technology Center  
ATTN: AIFRTA (Mr. Charles Ward)  
220 7th Street NE  
Charlottesville, VA 22901-5396
57. Dr. Mary F. Wheeler  
Department of Mathematical Sciences  
Rice University  
P. O. Box 1892  
Houston, Tx 77204-3476
58. Commander, U.S. Army Tank Automotive Command  
ATTN: AMSTA-RSK (Mr. Greg Wolfe)  
Bldg. 200  
Warren, MI 48317-5000
59. Director, Defense Nuclear Agency  
ATTN: RARP (Dr. Robert Young)  
6801 Telegraph Road  
Alexandria, VA 22310-3398
60. Office of the Assistant Manager for Energy  
Research and Development  
Department of Energy, Oak Ridge Operations  
P.O. Box 2001  
Oak Ridge, TN 37831
- 61-70. Office of Scientific and Technical Information  
P.O. Box 62  
Oak Ridge, TN 37830